Underground Target Extraction by Local Entropy Feature of Voxelized 3D Ground Penetrating Radar

Wenlong Wang [1] *, Qingwu Hu [1], Ju Zhang [2], Pengcheng Zhao [1], Mingyao Ai [1]

[1] Wuhan University, School of Remote Sensing, Wuhan, China - wangwenlong_rs@whu.edu.cn (WANG Wenlong); huqw@whu.edu.cn (Hu Qingwu);pengcheng.zhao@whu.edu.cn (Zhao Pengcheng);aimingyao@whu.edu.cn (Ai Mingyao);
[2] Wuhan City Polytechnic, School of Architecture and Engineering, Wuhan , China - zhangju@whu.edu.cn

Keywords: 3D Ground Penetrating Radar (3D GPR), voxelization, Underground Target Extraction, Local Entropy Feature.

Abstract

To solve the current problem of insufficient exploration of three-dimensional spatial information detected by 3D ground penetrating radar (3D GPR) and the data processing mainly based on the analysis and interpretation of two-dimensional slice images, a method is proposed to extract underground target based on the local entropy feature of discrete point clouds after the voxelization of 3D GPR data. First, the acquired 3D GPR data was voxelized into discrete three-dimensional point clouds. Then the local entropy feature of the voxelized point clouds over the entire region were calculated. The soil background and underground targets were distinguished by classifying them from multiple dimensions through Support Vector Machine (SVM). Finally, the urban road underground environment was taken as the research object, and this method was used for experimental analysis using measured data. The experimental results show that the accuracy of this method in extracting underground targets is as high as 90.1%, and the missing detection rate of missing underground targets is as low as 7.8%. The proposed method is accurate and effective, providing a new approach for 3D GPR to extract underground target.

1. Introduction

With the advancement of urbanization, the construction of roads, subways, pipelines and other underground structures projects has developed rapidly. Disasters such as road collapse also occur frequently. Ground penetrating radar is a remote sensing detection technology that uses the principle of different propagation characteristics of electromagnetic wave in different media to image the distribution of underground media (Qiu Yeji, 2015). Through the processing and interpretation of GPR underground detection data, it is possible to achieve the true restoration of underground media and non-destructive detection of abnormal media bodies, which provides technical support for remote sensing detection of underground physical spaces (Kim N et al., 2019). GPR has broad application prospects in the fields of urban underground pipeline detection, road disease detection (Shi Zhenshi, 2022), underground engineering structures (Cai Yihuang, 2019), archaeological excavation, and other fields.

In the early days, due to the limitations of GPR system hardware equipment technology, the data obtained by GPR were mainly one-dimensional single channel wave (A-Scan) or two-dimensional time profile (B-Scan) data. With the development of 3D GPR technology, the main data form of GPR has begun to become more accurate and intuitive three-dimensional image data (C-scan). Ground penetrating radar emits electromagnetic waves from a single transmitting antenna at the same time, and the reflected waves received are A-scan data, as shown in Figure 1 (a). B-scan data is the result of splicing multiple sets of A-scan reflection waves, as shown in Figure 1 (b). Ground penetrating radar emits electromagnetic waves by multiple transmitting antennas moving in the same direction for a certain distance within a certain period of time, while the corresponding receiving antennas receive the transmitted waves, obtaining multiple sets of B-scan data. These B-scan data are concatenated to obtain C-scan data, as shown in Figure 1 (c). C-Scan data is three-dimensional data collected by 3D GPR system, which is more intuitive and informative compared with A-Scan data and B-Scan data, presenting a complete three-dimensional space of the underground media (Ching G P H et al., 2021) .

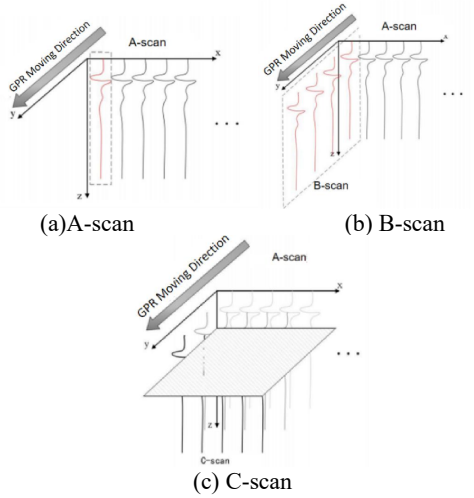

(a)A-scan (b) B-scan

(c) C-scan

Figure 1.Three types of GPR Data.

3D GPR has the advantages of high resolution, high signal-to-noise ratio, high acquisition speed, and more intuitive underground image data (Shi Lingfeng, 2008). With the development of GPR software and hardware technology and the demand for real underground three-dimensional spatial information, higher requirements have been put forward for the processing and analysis of three-dimensional ground penetrating radar data in practical applications. However, due to the fact that 3D GPR technology is still in the development stage, the collecting, processing and interpreting technology of 3D GPR data is not yet mature (Wang Dawei et al., 2023).

3D GPR collects C-scan data through a multi-channel three-dimensional antenna array, which can generate two-dimensional images such as vertical sections, cross sections, and horizontal

sections. These images can recognize target features from different angles. The current mainstream method for extracting underground target by 3D GPR is still based on the time-moment curve profile of two-dimensional slices of GPR (Yu kai and Zhang bin, 2011). This method is limited to the interpretation and analysis from two-dimensional perspective, and the basis for interpretation is very simple. Therefor, it cannot fully exploit the three-dimensional spatial characteristics of 3D GPR, and lacks further methods for extracting underground target using three-dimensional data. At present, the processing of C-scan data mainly involves generating horizontal slice images and establishing a data set of cracks, repairs, holes, and poor connections between layers for intelligent identification of diseases, or to use B-scan images and horizontal slices to establish a data set for small sample hole recognition. Another direction is to use a combination of three images, including one horizontal part and two vertical parts of C-scan data, as a training data set to improve classification accuracy.

At the same time, most of the existing 3D GPR experiments only collect underground data from a few sparse survey lines, and cannot synthesize three-dimensional data of the underground area (Hu Qunfang et al., 2020). Different from sparse lines, collecting and synthesizing three-dimensional data of 3D GPR and voxelizing the 3D GPR data can fully reflect the detailed conditions of the underground three-dimensional space. This method can identify the characteristics of underground targets from a three-dimensional perspective, thereby improving the extraction ability of underground targets (Zhang Wenbo et al., 2008).

2. Method of Extraction Underground Target by Voxelization and Local Entropy Feature

As shown in Figure 2, the overall process of this method is to preprocess the collected 3D GPR data first. The preprocessed 3D GPR data is then voxelized into discrete point cloud with three-dimensional coordinates and reflection feature values. Then calculate the local entropy features of the soil background and underground targets in the point clouds. Finally, the SVM is used to classify and optimize the parameters of local entropy features. The local entropy features are calculated based on the optimized parameters, and the underground targets are extracted through SVM.

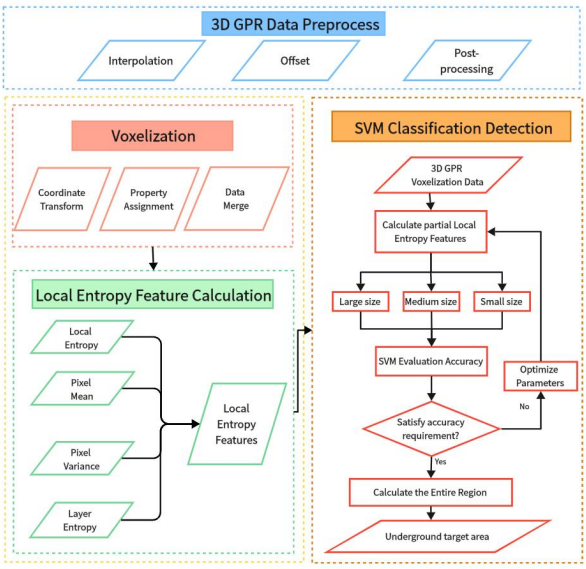

Figure 2. Method Flowchart.

2.1 Data Preprocessing

The purpose of ground penetrating radar data preprocessing is to reduce noise, enhance signal, improve signal-to-noise ratio, and extract correct amplitude, frequency, phase and other effective information from the data. The process is shown in Figure 3. The raw ground penetrating radar data must be preprocessed to obtain valid data with potential for further interpretation.

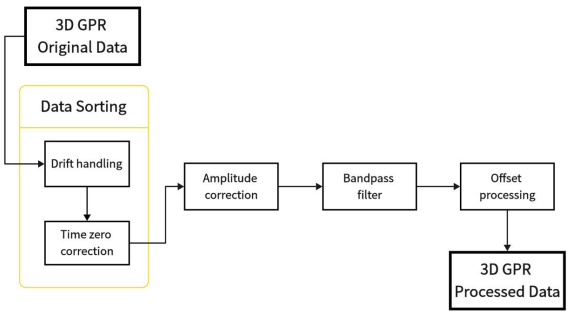

Figure 3. GPR Data Preprocessing Flowchart.

2.2 3D GPR data Voxelization

Voxelization converts the geometric form of a three-dimensional object into discrete point clouds represented by small cubic units. 3D ground penetrating radar data voxelization is the expansion of the two-dimensional image pixels of ground penetrating radar in three-dimensional space. The ground penetrating radar data is divided into small cubic blocks with a certain size and discrete coordinates. And specific attribute values are used to reflect its reflection characteristics (Ni Xuefei and Qin Fuchun, 2015). This method provides an effective means to interpret 3D ground penetrating radar data (Wang Xiurong et al., 2017). The process of 3D ground penetrating radar data voxelization is shown in Figure 4.

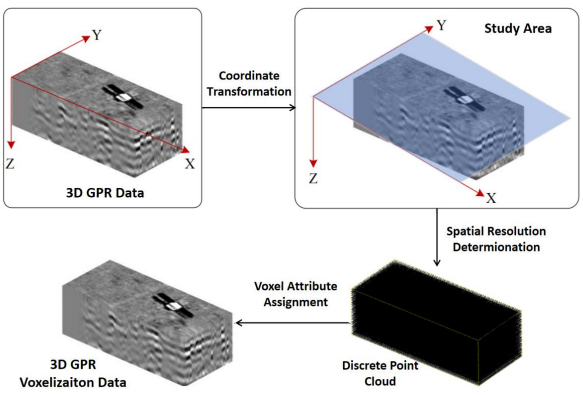

Figure 4. Voxelization Flowchart.

(1) Chunking and Layering: In order to reduce anomalies during the interpolation, the data is divided into several chunks and subjected to layering processing.

(2) Coordinate Transformation: Convert the position of each voxel unit to a unified coordinate system for data splicing.

(3) Spatial Resolution Determination: Calculate the x direction resolution *x0*, y direction resolution *y0*, and depth resolution *z0*. The horizontal resolution *x0* and *y0* are calculated based on the size of chunks. The depth resolution *z0* is the interval during layering in (1). Each voxel unit in the chunk represents 3D GPR data in the *x0* × *y0* × *z0* range.

(4) Voxel Assignment: In addition to three-dimensional spatial coordinates, 3D GPR data also records echo reflection feature information to reflect the distribution of underground media. Assign the reflection features from 3D ground penetrating radar data to the voxel units at the corresponding positions. Each voxel unit obtained after the final voxelization is completed has position information of X, Y, and Z coordinates and attribute information of reflection feature values.

(5)Result Merge: Splicing various rectangular chunks to obtain voxelization results of the entire detection area.

2.3 Local Entropy Feature Calculation

Local entropy reflects the amount of information contained in a local region (Wang Guangjun et al., 2000). The larger the local entropy *H* of this region, the greater the amount of information it contains, and the greater the probability of the existence of underground targets (Wang Yuanbin and Yin Yang, 2017). This article introduces the concept and calculation method of local entropy, and proposes the concept and calculation method of local entropy in three-dimensional regions, as shown in Figure 5.

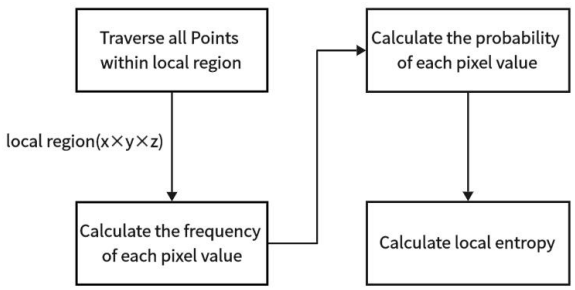

Figure 5. Local Entropy Feature Calculation Flowchart.

Traverse all points within the region x×y×z, obtain their pixel values and calculate their frequency. Then calculate the local entropy of the region as follows.

$$p(X=xi)=\frac{P(X=xi)}{\mathrm{x}\times\mathrm{y}\times\mathrm{z}}, \tag{1}$$

$$H(X)=-\sum_{x\in X}p(x)\log(p(x)), \tag{2}$$

where x×y×z = the size of the region
$X=\{0,1,2,\cdots,255\}$ = the range of pixel values
P(X=xi) = the frequency of pixel *xi* occurrence
p(X=xi) = the frequency of pixel *xi*
H(X) = the local entropy of the region

According to the experimental results of extracting underground targets based on local entropy, the accuracy of extracting underground targets solely through local entropy is relatively low. Therefore, based on local entropy, the pixel mean and pixel value variance of the region are calculated and added in local entropy features to enhance the ability to distinguish between soil background and underground targets.

$$\overline{X}=\frac{\sum X}{\mathrm{x}\times\mathrm{y}\times\mathrm{z}}, \tag{3}$$

$$D(X)=\frac{\sum(X-\overline{X})^2}{\mathrm{x}\times\mathrm{y}\times\mathrm{z}}, \tag{4}$$

where $\overline{X}$ = the pixel mean
D(X) = the pixel value variance

It should be noted that different types of underground targets have different extension directions, as shown in Figure 6 below. The red arrow in Figure 6 indicates the extension direction. Artificial vertical holes such as deep wells extend in the underground direction. However, underground pipes generally extend continuously in the horizontal direction. This difference in extension direction is reflected in the difference in local entropy feature changes of underground target point clouds in different directions. Underground targets and their general categories can be detected through the local entropy variance in each direction.In order to make full use of the three-dimensionality of 3D GPR, layer entropy variances in the three directions of x, y, and z are introduced into the local entropy feature to extract underground targets more effectively from a three-dimensional perspective.

$$D(H(X_x))=\frac{\sum_{x\in\mathrm{x}}(H(X_x)-\overline{H(X_x)})^2}{\mathrm{x}}, \tag{5}$$

$$D(H(X_y))=\frac{\sum_{y\in\mathrm{y}}(H(X_y)-\overline{H(X_y)})^2}{\mathrm{y}}, \tag{6}$$

$$D(H(X_z))=\frac{\sum_{z\in\mathrm{z}}(H(X_z)-\overline{H(X_z)})^2}{\mathrm{z}}, \tag{7}$$

where $D(H(X_x)), D(H(X_y)), D(H(X_z))$ = the layer entropy variance in the x, y, and z directions

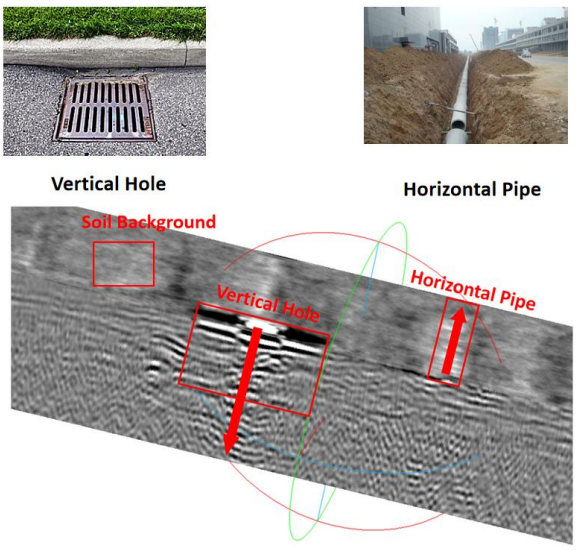

Figure 6. Extension Directions of Different Types of Underground Targets.

At the same time, different types of underground targets come in different sizes. Artificial vertical holes such as vertical boreholes penetrate several meters deep into the ground. This relatively large underground target is suitable for detection using a large local entropy feature calculation area. As shown in Figure 7, since the reflection feature value changes in the center area of a larger underground target have a certain thickness, if the area for calculating local entropy is too small, the center area of the underground target will not be detected. On the other hand, too small local entropy feature calculation area will also lead to excessive calculation and reduce the computational efficiency of extracting underground targets. Pipes are concentrated in shallow locations, and some are smaller in diameter. Some small holes and cracks on roads are also relatively small in spatial scale and these underground targets are suitable for detection using a smaller local entropy feature calculation area.

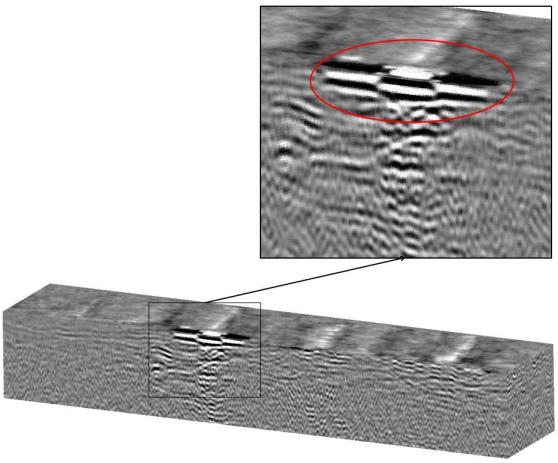

Figure 7. Large Underground Target Center Area Layering.

In order to better detect underground targets of different sizes and improve detection accuracy, this method uses three different sizes of local entropy calculation areas (x×y×z of Equation (1)) called large size, medium size and small size. The large size can reflect the entropy characteristics of a large area, but it is difficult to detect smaller underground targets, such as small pipelines. The small size can detect smaller targets, but compared to the large size, it is more susceptible to interference from local noise and then misdetection (Xue Fuguo, 2002). In order to improve the robustness of local entropy features of large, medium, and small sizes in underground target detection, detailed analysis and verification were carried out in experiments. On the other hand, in order to determine the optimal parameters for calculating local entropy features, such as the size of the calculation area of each size, the parameters should be adjusted according to the extraction results during the actual experiment.

2.4 SVM Underground Target Detection

Calculate the local entropy features of some soil background and various underground targets. Then optimize the local entropy feature parameters based on the classification results in the SVM. Finally, the local entropy features of the entire region are calculated, and the underground targets are extracted through SVM. The flowchart of this method is shown in Figure 8.

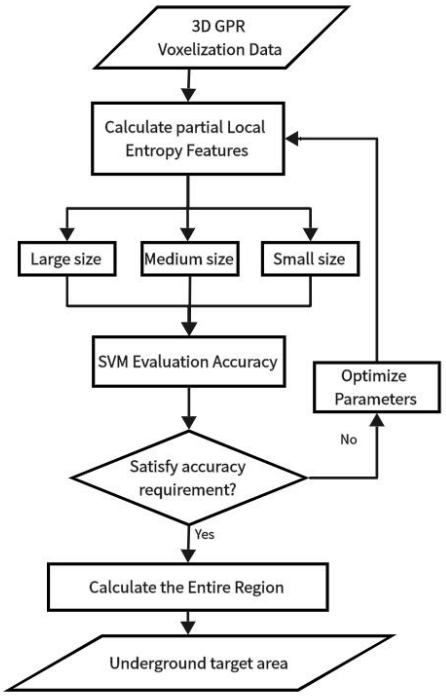

Figure 8. Underground Target extraction Based on Local Entropy Feature Flowchart.

The pseudocode of Detection implementation algorithm process is as follows:

Algorithm: Local entropy feature detection algorithm for underground targets

Input:

The whole region point cloud ρ ;
n-th local region point cloud ρ_n ;
Local entropy feature μ ;
Local entropy feature characteristic parameters β ;
Large, medium, and small size training sets $\varphi(\beta)$;
Classification accuracy threshold α_θ ;
Classification accuracy $\alpha_{\varphi(\beta)}$.

Output:

Underground target area (**UTA**)

While ($\alpha_{\varphi(\beta)} < \alpha_\theta$) **do**

optimize parameters β
calculate $\varphi(\beta)$
calculate $\alpha_{\varphi(\beta)}$ through SVM classification

Iterative optimization is performed to obtain local entropy feature parameters β and training set $\varphi(\beta)$ that meet accuracy requirements α_θ

While ($\rho_n < \rho$) **do**

Calculate local entropy $\mu_{\rho n}$
If SVM classification $\varphi(\beta)(\mu_{\rho n})$=1
$\rho_n \in$ Underground target area **UTA**

Output UTA;

3. Experiments and analysis

The handcart was equipped with a Raptor ground penetrating radar system for detection in the underground area of sports stadium ring road. The construction of underground structures in sports stadium is relatively regular, with clear types and characteristics of underground targets. Basic facilities such as pipelines and shafts are preserved, making it suitable for

conducting 3D ground penetrating radar underground target extraction experiments (Zhou Qicai et al., 2010). The orthophoto image of the experimental area is shown in Figure 9.

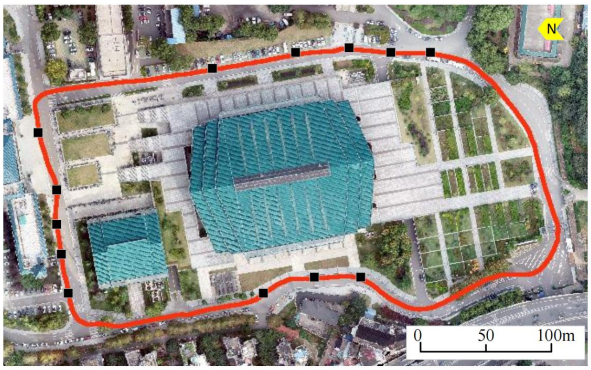

Figure 9. Orthophoto and Measurement Trajectory of the Experimental Survey Region.

3.1 Analysis of Voxelization Results

After collecting underground data from the sports stadium on the spot, the data of the entire study region was voxelized into three-dimensional point clouds according to the aforementioned voxelization method. The gray value of the point clouds correspond to the reflection feature values of underground media. As shown in Figure 10, the voxelization point cloud results of the underground target area: the underground target features are intuitive and clear, with high discrimination from the soil background. From a three-dimensional perspective, the grayscale values of the soil background do not show significant changes in all directions; the underground targets are more prominent and the gray value changes significantly in some direction; the artificial vertical holes appear black or white, extending deeper in the z-direction; the horizontal pipes extend horizontally and have grayscale values close to light white.

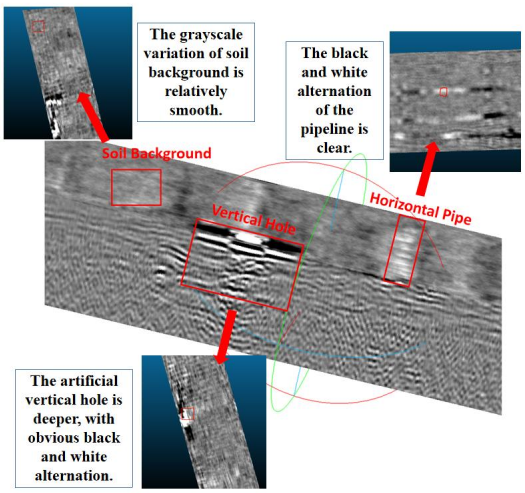

Figure 10. Voxelized Point Cloud Result of Some Region.

3.2 Local Entropy Feature Analysis

Select some soil background, underground targets and their edges, calculate and analyze their local entropy features. Some calculation and analysis results are shown in Table 1. Table 1 lists the local entropy features of 6 sample points a~f in three sizes: large, medium, and small, which all including entropy value, x-direction layer entropy variance, y-direction layer entropy variance, z-direction layer entropy variance, pixel mean, and pixel variance, all measured in pixel values 0~255.

	Serial Number	a	b	c	d	e	f
Large	Entropy Value	6.20	6.38	6.50	7.45	7.64	6.91
	x-Layer Entropy Variance	38.01	40.45	42.16	48.85	55.84	46.68
	y-Layer Entropy Variance	38.36	40.47	42.22	54.29	57.38	46.69
	z-Layer Entropy Variance	37.66	40.80	42.71	53.04	58.07	47.09
	Pixel Mean	128.00	127.00	127.00	127.00	127.00	127.00
	Pixel Variance	320.71	409.65	479.66	5431.55	2637.57	1035.28
Medium	Entropy Value	6.22	6.26	6.46	7.19	7.87	7.35
	x-Layer Entropy Variance	37.48	38.50	41.02	41.57	56.38	51.16
	y-Layer Entropy Variance	38.12	38.40	41.16	48.77	60.21	50.31
	z-Layer Entropy Variance	37.84	38.75	42.55	45.06	58.28	50.42
	Pixel Mean	126.00	126.00	127.00	130.00	125.00	130.00
	Pixel Variance	331.01	346.40	458.73	6862.81	4085.72	1991.75
Small	Entropy Value	6.26	5.86	6.49	7.11	7.87	7.72
	x-Layer Entropy Variance	36.38	32.79	39.19	36.62	52.90	50.81
	y-Layer Entropy Variance	36.70	32.30	39.43	42.68	53.99	48.98
	z-Layer Entropy Variance	36.72	32.64	42.17	37.93	50.78	48.27
	Pixel Mean	127.00	134.00	126.00	119.00	131.00	131.00
	Pixel Variance	357.33	251.63	492.86	7635.44	3984.92	3377.03

Table 1. Partial Local Entropy Feature Calculation Results

In Table 1, a, b, and c represent soil background, d and e represent artificial vertical holes, and f represents horizontal pipes.

As shown in Figure 11 and Table 1, the grayscale change of the soil background is relatively smooth; the entropy value is low; the pixel mean is close to 127; the pixel value variance is small. And the layer entropy variances in the x, y, and z directions are also small. Small size local entropy features have stronger robustness to soil background detection, but are more affected by noise at deeper positions, resulting in larger entropy values, layer entropy variance, and pixel variance of the soil background, which can easily lead to misjudgment.

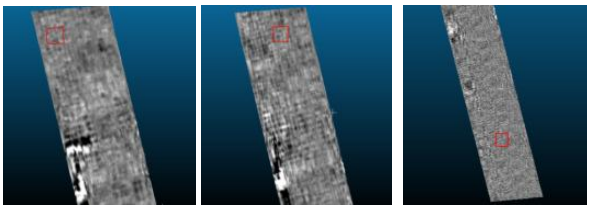

(a) (b) (c)

Figure 11. Soil Background Area.

As shown in Figure 12 and Table 1, the artificial vertical hole is deeper, with obvious black and white alternation. At the edge of the hole, the entropy value, layer entropy variance, and pixel variance are also significant. Large size local entropy features have stronger robustness. However, the layer entropy variance of small and medium sizes are greatly affected.

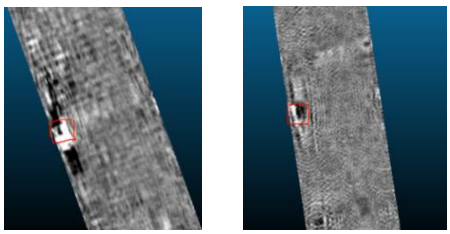

(d) (e)

Figure 12. Artificial Vertical Hole Area.

As shown in Figure 13 and Table 1, the pipeline is located in a shallower position with clear alternating black and white. Due to the small diameter of the pipeline, it is not suitable to use large size local entropy feature for detection. Under small size conditions, the entropy value, layer entropy variance, and pixel variance of the pipeline are relatively large, resulting in better detection performance for the pipeline.

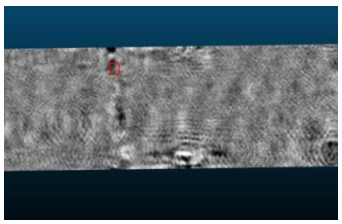

(f)

Figure 13. Horizontal Pipe Area.

3.3 Analysis of SVM Detection Results

According to the principle of uniform sampling, multiple background points and underground target points are extracted to calculate local entropy features. Use SVM for classification and ensure the classification accuracy reaches 95% through parameter optimization. Underground target area detection is performed based on the optimized parameters. And the detection results are compared with the true value labels to verify their accuracy. In order to integrate the advantages of local entropy features of different sizes, local entropy features of three sizes are used to synthesize feature vectors for classification. This method can not only reduce the interference of noise on underground target identification, but also detect relatively small underground targets. The comparison of original point cloud data and underground target acquisition results at small, medium, large and synthesis sizes is shown in Figure 14. The final and best detection result is shown in Figure 15 as follows.

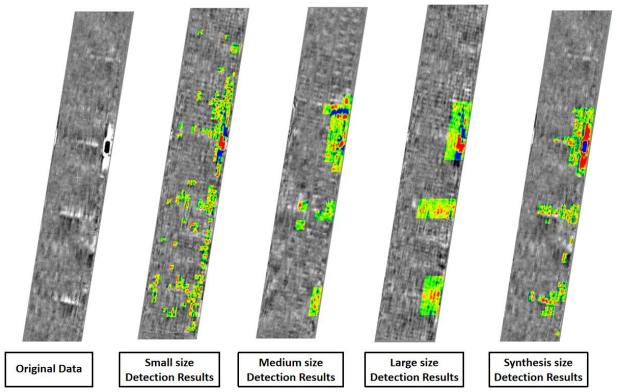

Figure 14. Comparison of Underground Target Extraction Results under Different Sizes.

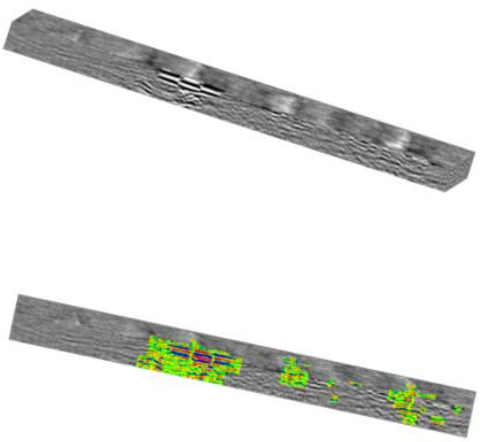

Figure 15. Underground target area extraction result.

As shown in Figure 16, the underground target detection results are overlaid with the drawn true value labels, and the underground target detection accuracy rate is calculated to be 90.1% and the missed detection rate is 7.8%. Local entropy features are less affected by noise, the detection accuracy of the underground targets is high, and the missed detection rate of underground targets is also low.

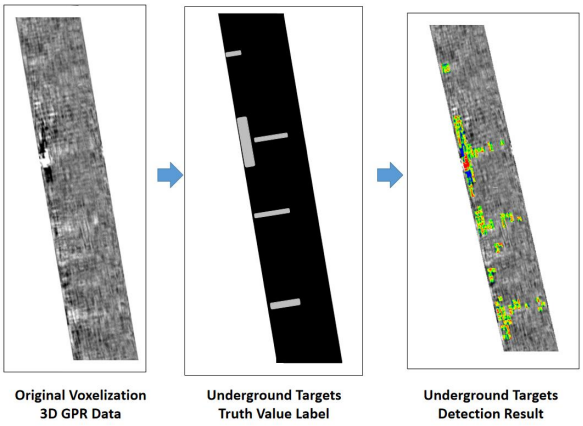

Figure 16. Underground Target Area Extraction Accuracy Calculation Flowchart.

Through classification by the trained SVM, the final accuracy and missing detection rate results of large size, medium size, small size and synthesis size are shown in Table 2. Large size detection of underground targets is more accurate, with an accuracy rate of 94.5%, but there are more missing underground targets, with a missing detection rate of 14%. There are fewer errors in underground targets of small size, with a low missing detection rate of 3.2%, but it is easier to detect soil background as underground targets, with a lower accuracy rate of 85.3%. Combining the three sizes of large, medium, and small can achieve both high accuracy and low missing rate, and obtain accurate and effective underground target detection results.

Size	Accuracy/%	Missing Rate/%
Large Size	94.5	14.0
Medium Size	89.7	9.6
Small Size	85.3	3.2
Synthesis Size	90.1	7.8

Table 2. Multi-size Detection Accuracy and Missed Detection Rate results

4. Conclusion

Currently ground penetrating radar is a hot field of scientific research, and 3D ground penetrating radar data processing is one of the hot spots among them (Li Jianing, 2014). This technology has been widely applied in geological exploration, tunnel engineering, underground pipelines and other fields. The rapid identification of underground targets has become an increasingly urgent demand.

This study aims at the problem that current 3D ground penetrating radar mainly focuses on detecting underground targets from two-dimensional segmented images, lacking the ability to extract underground targets from a three-dimensional perspective. This study proposes a method for extracting underground targets from a three-dimensional perspective, providing a high-precision and high-efficient solution for urban underground targets detection. This method has the characteristics of high accuracy, low missing rate, and automation without the need for manual interpretation.

This method innovatively adopts a new approach of interpreting and analyzing 3D ground penetrating radar data, converting 3D ground penetrating radar data into three-dimensional discrete point clouds. Accurately extract underground targets from the perspective of point clouds through the relationship between their three-dimensional positions and reflection feature values.

This method comprehensively considers the differences in the three-dimensional point cloud characteristics of soil background and underground targets, proposes local entropy features, and continuously supplements and optimizes local entropy features through experiments to improve the ability of local entropy features to distinguish soil background and underground targets. On the other hand, according to the characteristics of different underground targets, the robustness of identifying underground targets is enhanced from the perspective of multiple sizes.

However, there are still some issues with this method that need to be solved in future research. There is still room for further optimization of local entropy features; the data richness is insufficient to verify the robustness of the method in various complex situations; the processing of ground penetrating radar data still involves manual involvement, and achieving automation of ground penetrating radar data processing is one of the future research directions.

References

Cai Yihuang, 2019. Research on GPR-based pavement layering and road defect detection algorithm. Harbin Institute of Technology, Heilongjiang, China.

Ching G P H , Chang R K W , Luo T X H , et al. , 2021. GPR Virtual Guidance System for Subsurface 3D Imaging. *Remote Sensing*, 13(11):2154. doi.org/10.3390/rs13112154.

Hu Qunfang, Zheng Zhehao, Liu Hai, et al., 2020. Application of three-dimensional ground-penetrating radar in leakage detection of urban municipal pipelines. *Journal of Tongji University (Natural Science Edition)*, (7), 972-981. doi.org/10.11908/j.issn.0253-374x.19395.

Kim N , Kim S , An Y K , et al., 2019. A novel 3D GPR image arrangement for deep learning-based underground object classification. *International Journal of Pavement Engineering*, (2), 1-12. doi.org/10.1080/10298436.2019.1645846.

Li Jianing, 2014. Research on the application of Contourlet transform in the processing of ground-penetrating radar images of tunnel realisation. Chang’an University, Xi’an, China.

Ni Xuefei, Qin Fuchun, 2015. Internal and external somatotropic elements in human-fluid interaction simulation. *Science and Technology Perspectives*, (29), 133. DOI:CNKI:SUN:KJSJ.0.2015-29-099.

Qiu Yeji, 2015. Research on the application of deep learning in ground-penetrating radar data processing. Chang’an University, Xi’an, China.

Shi Lingfeng, 2008. Research on key technologies in ground-penetrating radar detection. Xidian University, Xi’an, China.

Shi Zhenshi, 2022. Optimisation of 3D ground-penetrating radar positioning and imaging accuracy for road subsidence hazards.

Guangzhou University, Guangzhou, China. doi.org/10.27040/d.cnki.ggzdu.2022.000171.

Wang Dawei, Lv Haotian, Tang Fujiao, et al., 2023. A Review of 3D Ground Penetrating Radar Road Hidden Disease Detection Analysis and Digitisation Techniques. *Chinese Journal of Highways*, 36(03), 1-19. doi.org/10.19721/j.cnki.1001-7372.2023.03.001.

Wang Guangjun, Tian Jinwen, Liu Jian, 2000. Detection of small targets in infrared images based on local entropy. *Infrared and Laser Engineering*, (4), 26-29. doi.org/10.3969/j.issn.1007-2276.2000.04.008.

Wang Xiurong, Len Guanggui, Niu Pengcheng, 2017. Research on the proposed seismic processing technology of 3D ground-penetrating radar data. *China Coal Geology*, 29(10), 70-75. doi.org/10.3969/j.issn.1674-1803.2017.10.12.

Wang Yuanbin,Yin Yang, 2017. An improved infrared weak target extraction method based on local features. *Infrared Technology*, (5), 414-420.

Xue Fuguo, 2002. Research on interest point detection and image matching techniques. Xi'an University of Electronic Science and Technology, Xi’an, China.

Yu Kai, Zhang Bin, 2011. Feasibility study of ground-penetrating radar for identification of physical parameters. *Western Prospecting Engineering*(12):170-171. doi.org/10.3969/j.issn.1004-5716.2011.12.060.

Zhang Wenbo, Wei Wenbo, Jin Jianen, et al., 2008. Detection of building structures using polarisation characteristics of ground-penetrating radar. *Journal of Jilin University (Earth Science Edition)*, (1), 156-160. DOI:CNKI:SUN:CCDZ.0.2008-01-024.

ZHOU Qicai, Chen Qiufeng, Jiang Shengnan, et al., 2010. Selection of operating parameters of ground-penetrating radar in shield forward detection application. *China Journal of Construction Machinery*, (3), 353-357. doi.org/10.3969/j.issn.1672-5581.2010.03.021.